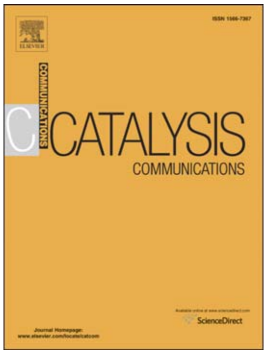

Ordered mesoporous copper oxide nanostructures as highly active and stable catalysts for aqueous click reactions

Seongwan Jang, Young Jin Sa, Sang Hoon Joo, Kang Hyun Park

PII: S1566-7367(16)30115-7
DOI: doi: 10.1016/j.catcom.2016.04.002
Reference: CATCOM 4625

To appear in: *Catalysis Communications*

Received date: 31 December 2015
Revised date: 31 March 2016
Accepted date: 6 April 2016

Please cite this article as: Seongwan Jang, Young Jin Sa, Sang Hoon Joo, Kang Hyun Park, Ordered mesoporous copper oxide nanostructures as highly active and stable catalysts for aqueous click reactions, *Catalysis Communications* (2016), doi: 10.1016/j.catcom.2016.04.002

Ordered mesoporous copper oxide nanostructures as highly active and stable catalysts for aqueous click reactions

Seongwan Jang[‡a], Young Jin Sa[‡b], Sang Hoon Joo[b,c,*], Kang Hyun Park[a,*]

[a] Department of Chemistry and Chemistry Institute for Functional Materials, Pusan National University, Busan 609-735, Republic of Korea

[b] Department of Chemistry, Ulsan National Institute of Science and Technology (UNIST), 50 UNIST-gil, Ulsan 689-798, Republic of Korea

[c] School of Energy and Chemical Engineering, Ulsan National Institute of Science and Technology (UNIST), 50 UNIST-gil, Ulsan 689-798, Republic of Korea

Seongwan Jang[‡a]

E-mail address: swjang@chemistry.or.kr

Young Jin Sa[‡b]

E-mail address: youngjinsa@unist.ac.kr

Sang Hoon Joo[b,c,*]

*Corresponding author. Tel: +82 52 217 2522, E-Mail address: shjoo@unist.ac.kr

Kang Hyun Park[a,*]

*Corresponding author. Tel: +82 51 510 2238, fax: +82 51 980 5200 E-mail address: chemistry@pusan.ac.kr

[‡] These authors contributed equally to this work.

Abstract: We demonstrate that ordered mesoporous CuO with gyroid mesostructures can be used as highly efficient, stable, and recyclable self-supported catalysts for click reactions in aqueous media.

Keywords: Nanostructures; Mesoporous materials; Copper; Click chemistry

1. Introduction

Click chemistry introduced by the work of Sharpless [1] and Meldal [2] is one of most efficient cycloaddition methods. This approach has attracted tremendous interests in various fields including material chemistry [3-5], combinatorial chemistry [6], and drug discovery [7]. The copper(I)-catalyzed azide-alkyne cycloaddition (ACC) reaction, one of the primary examples of click chemistry, proceeds in different solvents and yields stable triazoles with possible applications in DNA modification, as well as pharmaceutical and organic synthesis [8]. However, the instability of the Cu(I) species as manifested by the easy aerial oxidation of Cu(I) to Cu(II) has limited the application of Cu-catalyzed ACC reaction in other fields.

In the past years, many researches about AAC reactions catalyzed by Cu(II) catalyst have been investigated. In 2002, Sharpless and co-workers used $CuSO_4$ as catalyst for the ACC reaction with reductant [9]. In 2009, Zhu and co-workers used $Cu(OAc)_2$ catalyst in alcoholic solvent without reductants [10]; these authors also proved the reduction of Cu(II) to Cu(I) by alkynes during homocoupling reactions [11]. To improve catalytic activity of Cu(II) in ACC reactions, Kaboudin and co-workers reported Cu(II)-β-cyclodextric complex and this complex exhibited similar activity with previously reported Cu(I) catalyst in optimized condition [12].

To overcome the limitations of homogeneous catalytic systems, such as difficult catalyst recovery and low thermal stability, heterogeneous systems have been investigated as alternative catalysts [13-21]. The fabrication of porous nanostructures represents a promising approach to increase the catalytically active surface area and enhance the accessibility of the surface sites to the reactants, thereby enhancing the performance of heterogeneous systems [22,23]. Nanocasting represents one of the most successful strategies for fabricating ordered nanoporous materials. The nanoporous materials fabricated by this method show good thermal stability, high crystallinity, and highly ordered pore structures [24-26]. Particularly, the nanoporous materials templated from mesoporous silica with cubic gyroid structure such as KIT-6 are highly appealing, as their 3D-interconnected pore structure can provide highly accessible catalytically active surfaces, as well as structural stability during catalytic reactions. However, to our knowledge, no previous studies have investigated the use of copper(II) oxide nanoporous structures for click reactions.

Here we report for the first time high-performance heterogeneous catalysts for click reactions, based on ordered mesoporous copper(II) oxide (m-CuO) with 3D double gyroid mesostructure. The m-CuO catalysts showed high activity, recyclability, and excellent stability in the azide-alkyne cycloaddition reactions in aqueous media.

2. Experimental

2.1. Synthesis of ordered mesoporous copper(II) oxide nanostructures

Ordered mesoporous copper(II) oxide replica was synthesized by nitrate combustion method [27]. 1.9 g of $Cu(NO_3)_2 \cdot 3H_2O$ (Aldrich) was dissolved into 2.0 g of DI water, and 1.0 g of KIT-6 was added to the blue-coloured solution. The slurry was dried at 100 °C for 1 h. The silica-copper nitrate composite was placed with ammonia solution (28%, Samchun chemical) in a separate container, with a cover to prevent ammonia solution vapour dispersed through the atmosphere. Colour change was observed during this combustion step. After 1 h, the ammonia-treated composite was dried at 100 °C for 1 h, and subsequently added into a solution composed of 1.9 g of $Cu(NO_3)_2 \cdot 3H_2O$ and 3.0 g of DI water, and dried. Then, ammonia vapour treatment and drying were conducted. The dried powder was calcined at 400 °C for 6 h. (*Caution*: This calcination process explosively occurs, so using a wide crucible is highly recommended.) The resulting dark-grey compound was mixed with 0.1 M NaOH aqueous solution, and kept at 90 °C for 1 h to remove the silica template, then centrifuged at 4000 rpm for 10 min. These etching-centrifuging processes were repeated twice more, and the product was filtered, washed with DI water and ethanol, then dried at 60 °C.

2.2. General Procedure for Click Reactions

1.0 mg of m-CuO NPs (0.013 mmol, 1 mol%), benzylazide (0.15 mL, 1.26 mmol), phenylacetylene (0.195 mL,1.77 mmol), and 3.6 mL H_2O were placed in a 10 mL pressure schlenk tube. The reaction mixture was stirred at 50 ^{o}C. After 9 h, the reaction product analyzed by ^{1}H NMR using Varian Mercury Plus (300 MHz).

2.3. Recyclability Test

After the reaction, the catalyst particles were precipitated by centrifugation and washed with dichloromethane and ethanol. The particles were vacuum dried at room temperature and were used as a catalyst for another cycle of the reaction.

2.4. Catalyst characterization

X-ray diffraction (XRD) patterns of the samples were obtained by using a high-power X-ray diffractometer (D/Max 2500V/PC, Rigaku) with a Cu K_α source at 40 kV and 200 mA. Crystallite size of the framework particle of m-CuO was calculated by Scherrer equation.

$$\mathrm{D}_{hkl} = \frac{0.9\lambda}{(FWHM)\cos(\theta)}$$

D_{hkl} and λ, $FWHM$, and θ indicate crystallite size, wavelength of X-ray, full-width-half-maximum of a peak in radian, and Bragg angle respectively.

The pore structure was observed with a transmission electron microscope (TEM) (JEM-2100, JEOL) and high-resolution TEM (HR-TEM) (JEM-2100F, JEOL) at an acceleration voltage of 200 kV. The textural properties of the samples were obtained by N_2 physisorption analyzer (BELSORP-MAX, BEL) at -196 °C. Before measurements, the samples were evacuated with heating. Specific surface areas and total pore volumes were calculated by using the Brunauer-Emmett-Teller z(BET) equation in the relative pressure range of from 0.05 to 0.2. The pore size distributions were determined by the Barrett-Joyner-Halenda (BJH) method from the adsorption branch of the isotherm. X-ray photoelectron spectra (XPS) of the samples were collected by using K-alpha X-ray photoelectron spectrometer (Thermo Scientific).

3. Results and discussion

3.1. Structural characterization

The m-CuO nanostructures were synthesized by nanocasting with KIT-6 mesoporous silica with cubic *Ia3d* mesostructure (Fig. S1) [27]. In short, copper nitrate was infiltrated into the mesopores of KIT-6, and the nitrate was decomposed by vapor from the ammonia solution. A mesoporous CuO-silica composite was produced through calcination at 400 °C, and the silica template was then removed with hot dilute NaOH solution. The final m-CuO catalyst contained little amount of Si, which appears to be the residual silica template. The Si content determined by inductively coupled plasma-optical emission spectrometer was 6.0 wt%.

The transmission electron microscope (TEM) image of m-CuO (Fig. 1a) revealed a 3D double gyroid mesostructure, indicating the successful replication of the structure of the KIT-6 mesoporous silica template. The m-CuO framework thickness was around 10 nm. The lattice fringes clearly visible in the high resolution TEM (HRTEM) image of m-CuO (Fig. 1b) indicated the high crystallinity of the m-CuO framework. The distance between the two nearest lattices was 0.23 nm, commensurate with the *d*-spacing value between (111) planes of monoclinic CuO.

The structural integrity of the m-CuO investigated by small-angle X-ray diffraction (XRD) pattern (Fig. S2a) showed (211) and (220) reflections, indicating the preservation of cubic *Ia3d* symmetry after the replication. The high-angle XRD pattern of m-CuO (Fig. S2b) revealed that the CuO phase is consistent with monoclinic CuO (JCPDS 80-1268), confirming the HRTEM result. The crystallite size of CuO nanoparticles (calculated by applying the Scherrer equation to the (202) reflection) was 12.8 nm, in good agreement with the TEM observations. The textural properties of m-CuO were analyzed by nitrogen adsorption-desorption measurements. The isotherms in Fig. 2 clearly suggested the presence of mesopores in m-CuO, as evidenced by the hysteresis loop in the relative pressure range of 0.45–0.9. The m-CuO exhibited a large BET surface area of 248 m^2 g^{-1} and a total pore volume of 0.24 cm^3 g^{-1}. The pore size distribution of m-CuO obtained by the BJH method (Fig. 2, inset) revealed a predominant mesopore at 3.8 nm, along with a larger mesopore around 10 nm (indicated by an inverted blue triangle in the figure). The bimodal pore size distribution for m-CuO may facilitate mass transfer of reagents and products. The oxidation state of Cu species in m-CuO was accessed with Cu 2p X-ray photoelectron spectrum (Fig. 3). The strong satellite peak accompanying the $2p_{3/2}$ peak rules out the presence of the Cu_2O phase [28]. Interestingly, the binding energy of the Cu $2p_{3/2}$ peak in m-CuO (~937 eV) was higher than that for bulk CuO (933–934 eV), and the peak was broader. The shift in the Cu $2p_{3/2}$ peak can be attributed to the nanoscale size of the m-CuO framework, which could expose a large number of Cu atoms on its surface [29-30].

3.2. Catalytic activity of the catalysts

We next explored the catalytic properties of m-CuO in the AAC reactions. In order to assess the effect of the solvent, we carried out the AAC reaction of benzyl azide and phenylacetylene in various solvents (entries 1–5, Table 1). The conversion of benzyl azide was much higher in protic than in aprotic solvents. Generally, water is a poor solvent for most click reactions. To improve catalytic activity of nanoparticles in aqueous media, supporting material and/or surfactant were extensively used [28]. Xia groups reported the CuO catalyst supported by polymeric ionic liquid material for AAC reactions in water [31]. Also, Kong groups reported the Cu_2O catalyst coated by water-soluble polymer such as polyvinylpyrrolidone [32]. Very similarly, the obtained our m-CuO exhibited remarkably enhanced AAC catalytic activity in water.

Therefore, we used water as solvent in the subsequent reactions, for both economic and environmental reasons. The catalytic activity of the m-CuO catalyst was almost six times higher than that of a commercial catalyst used for comparison, and 20 times higher than without catalyst (entries 5–7, Table 1). This difference can probably be attributed to the large specific surface area and pore volume of m-CuO. The AAC reactions carried out with m-CuO as catalyst showed increased reactivity with increasing temperature (entries 5 and 8–9, Table 1). The recovered catalyst could be reused at least three times without loss of catalytic activity and selectivity (entries 10–11, Table 1). Compared to the original mesoporous nanostructure, the catalyst did not show significant structural damage after recycling three times (Fig. S3a). Furthermore, the original lattice fringes were maintained in the recycled nanoparticles (Fig. S3b).

The accepted reaction mechanism for the AAC reaction catalyzed by copper ions is depicted in Fig. S4. [33] In the first step, one of copper ion forms a π-complex with the alkyne. Then, copper acetylide is generated by replacing the proton with another copper ion.

The scope of the reaction was examined for various alkynes and azides (Table 2). Moderate conversions of these substrates were obtained under the optimized conditions. As shown in entries 1–6 of Table 2, the electronic properties of both azides and alkynes significantly influenced the consequence of the reaction. For example, 4-bromophenyl acetylene (entry 1, Table 2) and 4-fluorobenzyl azide (entry 4, Table 2) substituted with an electron-withdrawing group showed lower reactivity than compounds substituted with an electron-donating group (entries 2–3 and 5–6, Table 2). This is deemed the results of decreasing of nucleophilicity of the acetylide anion and efficiency of cyclization step with triazenide decreased by substitution with electron-withdrawing groups. The reactivity of methoxyphenyl azides substituted in *para*-, *meta*-, and *ortho*- position was also assessed (entries 6–8, Table 2). The *ortho*- substituent yielded the lowest conversion, due to interference with the ring closure of the intermediate [34]. Unexpectedly, the *para*-substituent showed lower reactivity than the *meta*- one, even though it represents the best activating site in a number of click reactions. We also examined the reactivity in relation to the length of the chain directly linked to the reactive azide (entries 9–10, Table 2). While phenyl and benzyl azides showed high conversion within 9 h, 2-phenylethyl azide required more than 18 h for achieving a similar conversion. This result seems to reflect the rapidly increasing interference with increasing steric hindrance.

4. Counclusions

In conclusion, m-CuO nanostructures were synthesized through nanocasting from KIT-6 mesoporous silica with cubic *Ia3d* mesostructure, and employed as self-supported catalysts for the ACC reactions. The m-CuO catalysts showed high catalytic activity in water, and were suitable for multiple reuses. Therefore, m-CuO catalysts are able to balance reactivity, robustness, and environmental compatibility of aqueous click reactions.

Acknowledgements

This research was supported by Basic Science Research Program through the National Research Foundation of Korea (NRF) funded by the Ministry of Science, ICT & Future Planning (NRF-2015R1D1A1A02060684 and NRF-2013R1A1A2012960).

References

[1] H.C. Kolb, M.G. Finn, K.B. Sharpless, Angew. Chem. Int. Ed. 40 (2001) 2004-2021.
[2] C.W. Tornoe, C. Christensen, M. Meldal, J. Org. Chem. 67 (2002) 3057-3064.
[3] N.K. Devaraj, G.P. Miller, W. Ebina, B. Kakaradov, J.P. Collman, E.T. Kool, C.E.D. Chidsey, J. Am. Chem. Soc. 127 (2005) 8600-8601.
[4] K. Kempe, A. Krieg, C.R. Becer, U.S. Schubert, Chem. Soc. Rev. 41 (2012) 176-191.

[5] W. Xi, T.F. Scott, C.J. Kloxin, C.N. Bowman, Adv. Funct. Mater. 24 (2014) 2572-2590.

[6] D.B. Ramachary, C.F. Barbas, III, Chem. - Eur. J. 10 (2004) 5323-5331.

[7] H.C. Kolb, K.B. Sharpless, Drug Discovery Today 8 (2003) 1128-1137.

[8] J.E. Moses, A.D. Moorhouse, Chem. Soc. Rev. 36 (2007) 1249-1262.

[9] V.V. Rostovtsev, L.G. Green, V.V. Fokin, K.B. Sharpless, Angew. Chem. Int. Ed. 41 (2002) 2596-2599.

[10] W.S. Brotherton, H.A. Michaels, J.T. Simmons, R.J. Clark, N.S. Dalal, L. Zhu, Org. Lett. 11 (2009) 4954-4957.

[11] G.-C. Kuang, P.M. Guha, W.S. Brotherton, J.T. Simmons, L.A. Stankee, B.T. Nguyen, R.J. Clark, L. Zhu, J. Am. Chem. Soc. 133 (2011) 13984-14001.

[12] B. Kaboudin, Y. Abedi, T. Yokomatsu, Org. Biomol. Chem. 10 (2012) 4543-4548.

[13] Z.-c. Zhang, B. Xu, X. Wang, Chem. Soc. Rev. 43 (2014) 7870-7886.

[14] Y. Zhang, X. Cui, F. Shi, Y. Deng, Chem. Rev. (Washington, DC, U. S.) 112 (2012) 2467-2505.

[15] J. Shi, Chem. Rev. (Washington, DC, U. S.) 113 (2013) 2139-2181.

[16] H. Woo, H. Kang, A. Kim, S. Jang, J.C. Park, S. Park, B.-S. Kim, H. Song, K.H. Park, Molecules 17 (2012) 13235-13252.

[17] G. Zhao, J. Wang, X. Peng, Y. Li, X. Yuan, Y. Ma, Chem. - Asian J. 9 (2014) 546-553.

[18] M. Biswas, A. Saha, M. Dule, T.K. Mandal, J. Phys. Chem. C 118 (2014) 22156-22165.

[19] A. Berrichi, R. Bachir, M. Benabdallah, N. Choukhou-Braham, Tetrahedron Lett. 56 (2015) 1302-1306.

[20] A. Saha, D. Saha, B. Ranu, Org. Biomol. Chem. 7 (2009) 1652-1657.

[21] J. Chen, J. Qi, G. Li, F. Zheng, S. Li, Z. Tang, Chem. – Asian J. 8 (2013) 694-699.

[22] N. Linares, A.M. Silvestre-Albero, E. Serrano, J. Silvestre-Albero, J. Garcia-Martinez, Chem. Soc. Rev. 43 (2014) 7681-7717.

[23] V. Valtchev, L. Tosheva, Chem. Rev. (Washington, DC, U. S.) 113 (2013) 6734-6760.

[24] B. Tian, X. Liu, H. Yang, S. Xie, C. Yu, B. Tu, D. Zhao, Adv. Mater. (Weinheim, Ger.) 15 (2003) 1370-1374.

[25] D. Han, D. Li, T. Zheng, Adv. Mater. Res. (Zuerich, Switz.) 15-17 (2007) 53-58.

[26] K. Jiao, B. Zhang, B. Yue, Y. Ren, S. Liu, S. Yan, C. Dickinson, W. Zhou, H. He, Chem. Commun. (Cambridge, U. K.) (2005) 5618-5620.

[27] Y. Ren, Z. Ma, L. Qian, S. Dai, H. He, P.G. Bruce, Catal. Lett. 131 (2009) 146-154.

[28] D. Barreca, A. Gasparotto, E. Tondello, Surf. Sci. Spectra 14 (2008) 41-51.

[29] K. Borgohain, J.B. Singh, M.V. Rama Rao, T. Shripathi, S. Mahamuni, Phys. Rev. B: Condens. Matter Mater. Phys. 61 (2000) 11093-11096.

[30] Z.-s. Hong, Y. Cao, J.-f. Deng, Mater. Lett. 52 (2002) 34-38.

[31] Y. Wang, J. Liu, C. Xia, Adv. Synth. Catal. 353 (2011) 1534-1542.

[32] Z. Zhang, C. Dong, C. Yang, D. Hu, J. Long, L. Wang, H. Li, Y. Chen, D. Kong, Adv. Synth. Catal. 352 (2010) 1600-1604.

[33] B. T. Worrell, J. A. Malik and V. V. Fokin, Science 340 (2013) 457–460.

[34] S.W. Kwok, J.R. Fotsing, R.J. Fraser, V.O. Rodionov, V.V. Fokin, Org. Lett. 12 (2010) 4217-4219.

Figure Captions

Fig. 1. (a) TEM and (b) HRTEM images of m-CuO nanostructures

Fig. 2. N_2 adsorption-desorption isotherms of m-CuO and the corresponding pore size distribution (inset).

Fig. 3. Cu 2p XPS spectrum of m-CuO sample.

Table 1. Optimization of click reactions catalyzed by m-CuO.

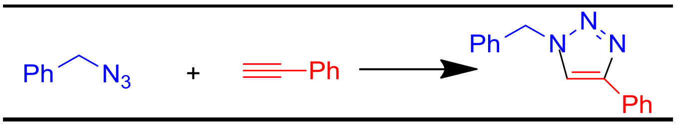

Entry	Cat. (mol%)	Solvent	Temp. (ºC)	Time (h)	Yield[a](%)
1	5	H_2O/t-BuOH(2:1)	50	12	56
2	5	t-BuOH	50	12	8
3	5	DMSO	50	12	15
4	5	CH_3CN	50	12	85
5	1	H_2O	50	9	>99
6	1 [b]	H_2O	50	9	16
7	-	H_2O	50	9	5
8	1	H_2O	25	9	24
9	1	H_2O	40	9	65
10	Recovered #5	H_2O	50	9	>99
11	Recovered #12	H_2O	50	9	>99

Reagents and conditions: benzyl azide, 1.26 mmol; phenylacetylene, 1.77 mmol. [a] Determined by ^{1}H-NMR. Yields are based on the amount of benzyl azide used. [b] Commercial CuO purchased from Aldrich (cat. no. 544868).

Table 2. Click reactions of various azides with terminal alkynes catalyzed by m-CuO.

Entry	Azide	Alkyne	Time (h)	Yield[a] (%)
1	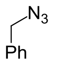	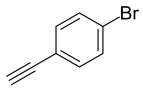	9	62
2	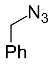	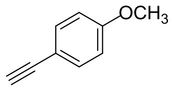	9	97
3	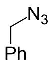	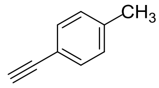	9	100
4	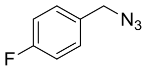	≡—Ph	9	72
5	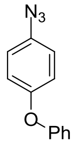	≡—Ph	9	98
6	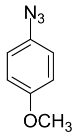	≡—Ph	9	85
7	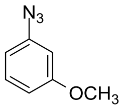	≡—Ph	9	96
8	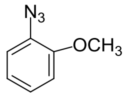	≡—Ph	9	72
9	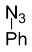 N_3 Ph	≡—Ph	9	98
10	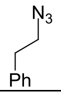	≡—Ph	18	85

Reagents and conditions: azide, 1.26 mmol; alkyne, 1.77 mmol; water, 3.6 mL; catalyst, 1 mol %; temperature, 323 K. [a] Determined by ^{1}H-NMR. Yields are based on the amount of azide used.

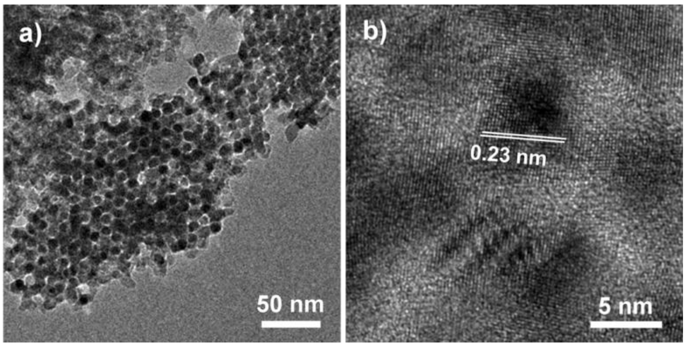

Fig. 1

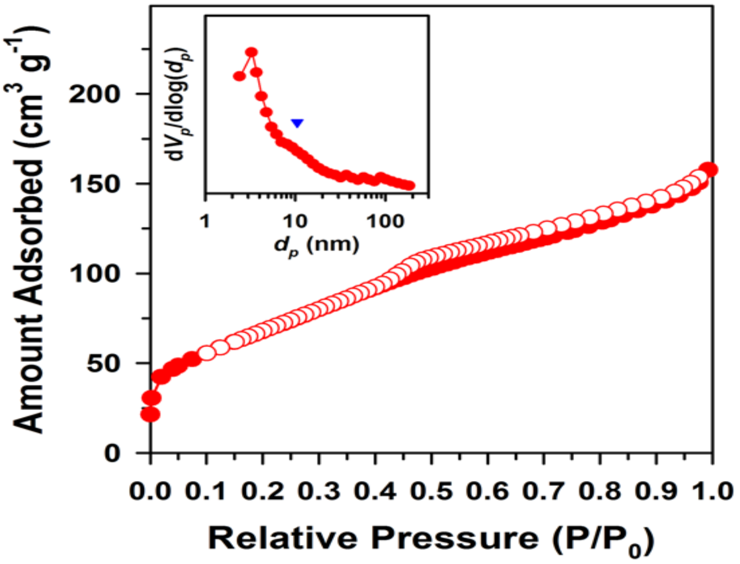

Amount Adsorbed (cm^3 g^{-1})
0
50
100
150
200
0.0 0.1 0.2 0.3 0.4 0.5 0.6 0.7 0.8 0.9 1.0
Relative Pressure (P/P$_0$)
dV$_p$/dlog(d$_p$)
1
10
100
d$_p$ (nm)

Fig. 2

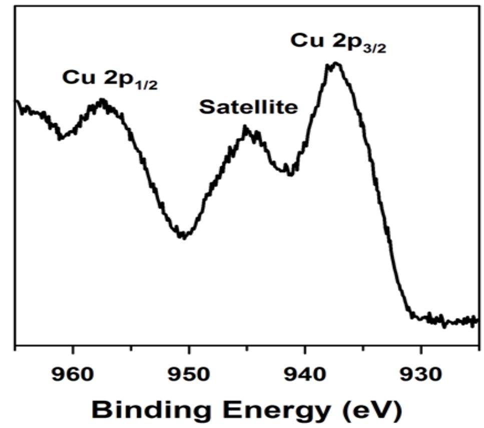

Fig. 3

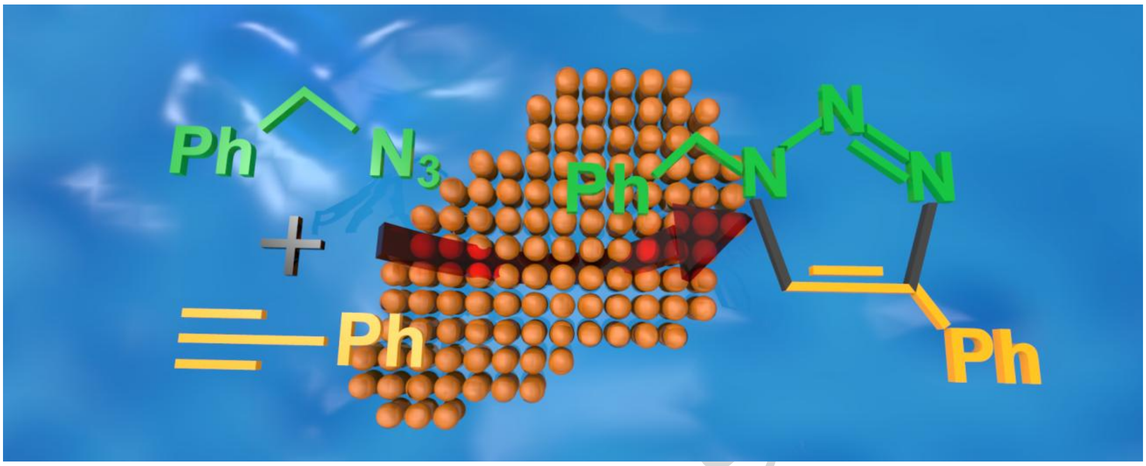

Graphical abstract

Highlights

- The m-CuO catalysts were synthesized by nanocasting with KIT-6 mesoporous silica.
- The m-CuO showed high catalytic activity for click reactions in aqueous media.
- The recovered catalyst could be reused without loss of the activity and selectivity.